**Supplemental Figure 1. Structural Features of p.Gly23Val-MRAS after Twenty Nanosecond Molecular Dynamic Simulations**

The corresponding conformations of WT-MRAS (white) vs. p.Gly23Val-MRAS (red) were compared after superimposition using the best RMSD. Circles denote the regions of the protein which the mutation-associated remodeling leads to the State I-to-State II transition, namely Switch I (blue) and Switch II (green). These changes in secondary structure are responsible of the remodeling in the active site and the exposure of surfaces for protein-protein interactions.

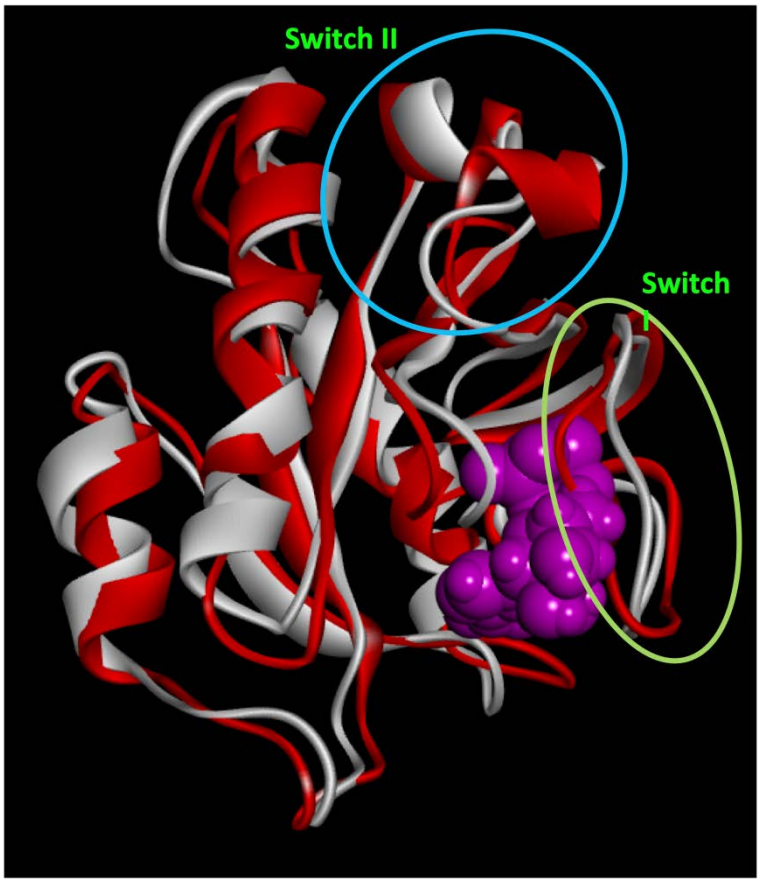

**Supplemental Figure 2. Remodeling of p.Gly23Val-MRAS after Molecular Dynamic Simulations Cause Exposure of Distinct Interphase Surfaces for Interaction with Effectors**

Comparative surface analyses were performed for WT-MRAS (yellow) and p.Gly23Val-MRAS (red) following molecular dynamic simulations. p.Gly23Val-MRAS displays surface changes, particularly at the Switch I (green circle) and II (light blue circle) regions and near the nucleotide (turquoise) binding site. Graphics display the water-accessible surface.

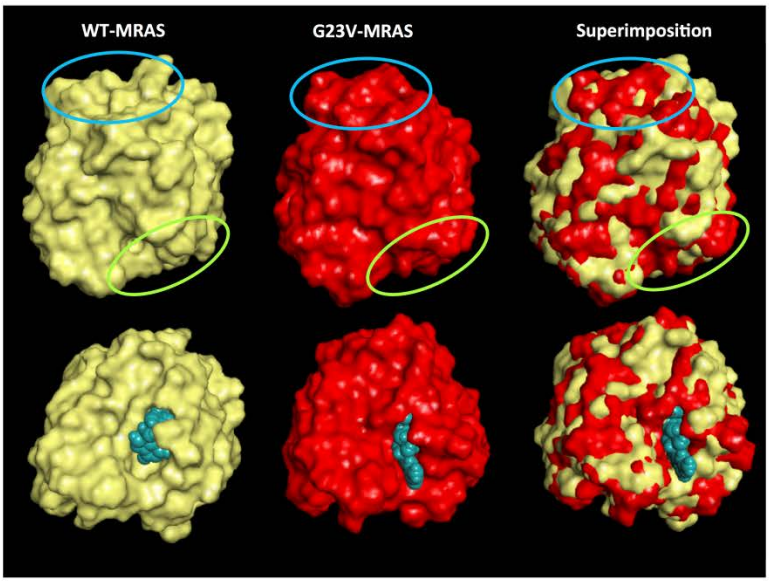

**Supplemental Figure 3. Clinical Phenotype of Patient Harboring p.Thr68Ile-MRAS mutation.**

A) The patient at 20 months of age shows sparse hair, tall forehead, apparent hypertelorism and mild ptosis.

B) The patient at 6 years of age shows thick hair, apparent hypertelorism, mild ptosis, low-set, posteriorly rotated ears and pointed chin.

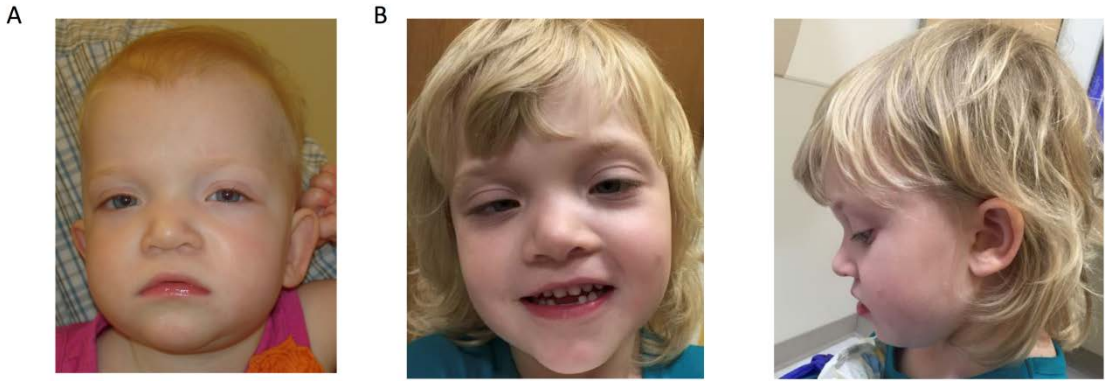

**Supplemental Figure 4. Molecular Modeling of Human WT-MRAS and the Patient's p.Gly23Val-MRAS**

A) The homology-based model of human MRAS, derived from the structure of murine MRAS as a template.

B) The model of p.Gly23Val-MRAS was generated by in vitro mutagenesis.

C) The Ramachandran plot performed after energy minimization, for the homology-derived human WT-MRAS protein displays more than 97% of residues within the allowed regions.

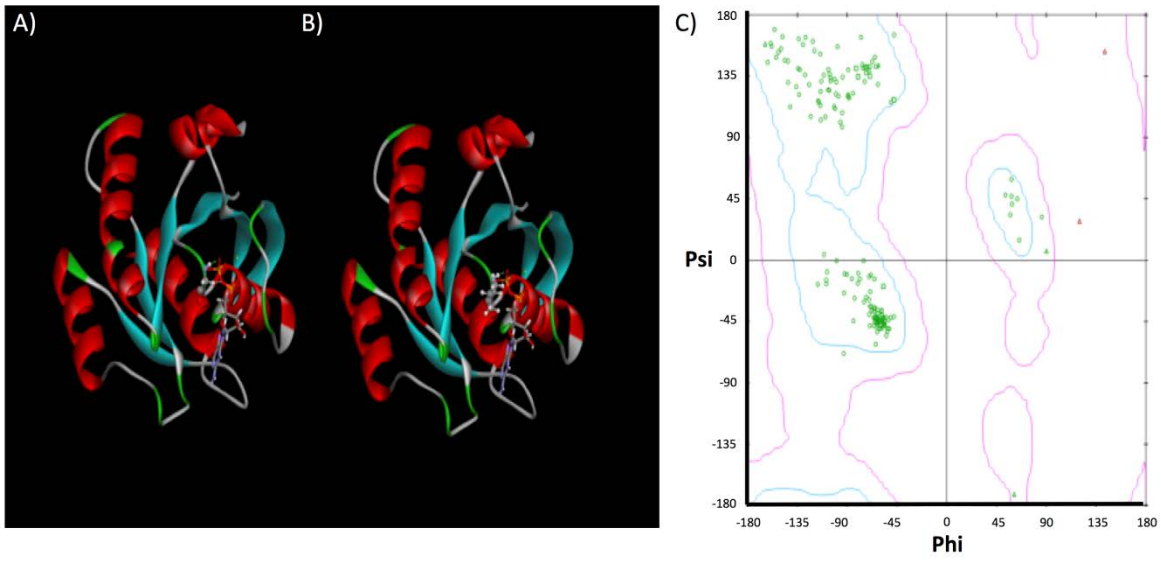

**Supplemental Table 1.** *In Silico* Analyses of Patient Derived Variants

| Tool | G23V-MRAS | C25G-MICAL2 | R559Q-MICAL2 |
|---|---|---|---|
| **PolyPhen2** | Probably damaging | Probably damaging | Possibly damaging |
| **Provean** | -8.24 (deleterious) | -10.87 (deleterious) | -3.57 (deleterious) |
| **SIFT** | 0.000 (damaging) | .001 (damaging) | 0.093 (tolerated) |
| **Mutation Assessor** | 3.56 (high) | 3.155 (medium) | 3.12 (medium) |
| **Fathmm** | -1.77 (damaging) | 1.04 (tolerated) | -3.55 (damaging) |
| **Align GVGD** | 109.55 (C65) | 158.23 (C65) | 42.81 (C35) |

**Supplemental Table 2**. Oligonucleotide Primers for Mutational Analysis of *MRAS*

| Exon | Forward primer (5'-3') | Reverse primer (5'-3') |
|---|---|---|
| **2** | AGCCCTCTGTCTCATTCCA | CCCCACTGAAACCTGTCAA |
| **3** | GCAGCAGTGTTGGAGTCTT | GCAGGCCTCTTCCCGGTA |
| **4** | TGGGCTGGCTGTGCTATG | TGACCAGGCTACAGCTTTTA |
| **5** | TGGGCATTTTTAAGGGTGTAA | TGTGGAGGCCCGCTTCTA |
| **6** | TGGGGCTAGGGAGGAGAG | GGGCCAAGGGTTGTGGTTA |